Cytometry PART A
Journal of the International Society for Advancement of Cytometry

MIFlowCyt

Cell Surface Markers and Exogenously Induced PpIX in Synovial Mesenchymal Stem Cells

Jaroslav Denkovskij,[1]* Romualdas Rudys,[2] Eiva Bernotiene,[1] Mindaugas Minderis,[3] Saulius Bagdonas,[4] Gailute Kirdaite[2]

[1]Department of Regenerative Medicine, State Research Institute Centre for Innovative Medicine, Vilnius, 01102, Lithuania

[2]Department of Innovative Technologies for Diagnostics, Treatment and Health Monitoring, State Research Institute for Innovative Medicine, Vilnius, 01102, Lithuania

[3]Faculty of Medicine, Clinic of Rheumatology, Traumatology-Orthopaedics and Reconstructive Surgery, Vilnius University, Vilnius, LT-08661, Lithuania

[4]Laser Research Center, Faculty of Physics, Vilnius University, Vilnius 10222, Lithuania

Grant sponsor: Research Council of Lithuania, Grant number: MIP-121/2010

Additional Supporting Information may be found in the online version of this article.

*Correspondence to: Jaroslav Denkovskij; State Research Institute Centre for Innovative Medicine, Zygimantu 9, 01102, Vilnius, Lithuania. E-mail: jdenkovskij@yahoo.com

Published online 10 September 2015 in Wiley Online Library (wileyonlinelibrary.com)

DOI: 10.1002/cyto.a.22781

Abstract

The aim of present study was to assess the expression of surface markers and the accumulation of protoporphyrin IX in synovial mesenchymal stem cells (SMSCs). SMSC from patients with rheumatoid arthritis (RA, $n = 5$) and osteoarthritis (OA, $n = 5$–6) were characterized and their PpIX accumulation rates were evaluated by flow cytometry. The expression of the 21 out of 24 tested surface markers, related to stem-like features and aggressiveness of cells showed no statistically significant differences between RA and OA groups. However, the cells from RA group had the significantly lower levels of expression for the integrin-associated protein CD47 and the grow factor receptor CD271 ($P = 0.018$), while the higher levels of cell membrane zinc-dependent metalloproteinase CD10 ($P = 0.006$), as compared to the cells from OA group. Comparison of the mean intensities of PpIX fluorescence revealed no statistically significant differences between the RA and OA groups, as well as no relation to proliferation rates or cell size, although some conspicuous distinction in PpIX accumulation was observed in certain specimens within these groups, suggesting possibilities of this method application for characterization of individual SMSC populations. CD10, CD47, and CD271 were differently expressed in RA and OA SMSC, while had no direct association with the PpIX fluorescence intensity.

Key terms

Arthritis; cell surface markers; protoporphyrin IX; synovial mesenchymal stem cells

THE hallmarks of rheumatoid arthritis (RA) pathology are chronic inflammation and pronounced synovial hyperplasia. The synovial tissue is composed of a variety of cell types: type A cells (macrophages), type B cells (fibroblast-like cells), adipocytes, mast cells, and vascular endothelial cells. The central feature of synovitis in RA is transformation of fibroblast-like synovial cells (FLS) into autonomously proliferating cells that play a key role in expressing variable levels of adhesion molecules, secreting distinct patterns of cytokines, and forming hyperplastic tissue with potential to induce bone erosion and cartilage degradation known as pannus (1,2). The abnormal phenotypes of these cells have ability to spread RA to unaffected joints and express variety of features typical for multiple synovial inflammation (3,4). There have been attempts to explain such phenotype of RA FLS by activation of normal FLS through accumulation of genetic and epigenetic abnormalities, similar to those occurring in cancer (5). However, not all fibroblasts in a joint become activated and influence the pannus formation. There is growing evidence that RA is a heterogeneous disease (6), progression of which, besides other types of cells, involves mesenchymal stem cells (MSC) (7). MSC can be isolated from the synovial membrane by the same protocol as for synovial fibroblasts, suggesting that MSC correspond to a subset of the adher-

ent synovial cell population. This RA FLS population showed differentiation potential, survival, and immunophenotypic characteristics similar to those of normal MSC, however, possessed impaired clonogenic and proliferative potential with premature telomere length loss (8). It is also thought that highly inflammatory milieu in arthritic joints may induce and maintain the dynamic changes of MSC properties that may cause subsequent transformation of these cells involving them in synovitis processes leading to pannus formation (9).

Despite recent progress in the field of RA pathogenesis, where the main attention is paid to characterisation of FLS, the role of MSC in the rheumatic diseases remains largely unknown. Therefore, to get a broader insight on characteristics of synovial MSC (SMSC), we analyzed the expression pattern of surface markers associated with aggressive behavior and stem-like features of the synovial MSC in relation to their metabolic activity. The inflamed synovium of RA exhibits many characteristics typical for malignant tissues such as hypermetabolic activity and extensive neovascularization (10). For estimation of cell metabolic activity, we followed the accumulation of endogenous protoporphyrin IX (PpIX), which is commonly used for the photodetection of malignant tissue (11), considering SMSC size and proliferation rate. It has been shown that after the application of exogenous 5-aminolevulinic acid (5-ALA) tissues with a pronounced metabolic turnover, such as proliferating blood vessels or cancerous tissues, accumulate higher amounts of endogenous photosensitizer PpIX (12) during the natural process of haem biosynthesis, which takes place in the mitochondria. Our previous findings demonstrated that the PpIX accumulation in inflamed synovial tissues was higher than in corresponding control tissues (10,13,14). Since the correlation between PpIX accumulation and malignancy has been reported (15), we tested the relation between PpIX accumulation and the expression of the cell surface markers of aggressiveness in populations of SMSC.

Methods and materials

SMSCs Cultures

Samples of synovium were obtained as postoperative tissues during articular replacement surgery from patients with osteoarthritis (OA) group ($n = 6$) and RA group ($n = 5$) (Lithuanian Bioethics Committee permission No. 158200–12-270-63). The diagnosis of OA conformed to the American College of Rheumatology criteria for the knee (16); RA patients fulfilled the American College of Rheumatology revised criteria (17). The specimens of patients with OA were collected from the knee joint and those of patients with RA—from the small joints of the hand. SMSC were isolated from the postoperative specimens of synovial tissues. Minced synovial tissues were incubated overnight in Dulbecco's modified eagle medium (DMEM) (with 1 g/L D-glucose, sodium pyruvate, L-Glutamine, phenol red; Invitrogen: 21885025) without fetal bovine serum (FBS) in a humidified 5% CO_2 incubator at 37°C. After incubation synovial tissues were digested with 0.1% collagenase (Type I, Biochrom, C 1–22) in DMEM and the isolated cells were cultured in 75-cm^2 culture flasks in DMEM supplemented with 10% FBS (Biochrom, S0615), and 1% stock solution of penicillin (10,000 units/mL), streptomycin (10 mg/mL), and amphotericin B (0.025 mg/mL, Biological Industries, 03–033-1B). At 95% confluence, the adherent synovial cells were passaged by digestion with 0.25% trypsin/0.2% ethylenediaminetetraacetic acid (EDTA) (Biological Industries, 03–050-1) and used between passages 2 and 4 for all experiments. Cells were plated into 75-cm^2 culture flasks in DMEM containing 10% FBS. Typical profile for MSC surface markers and the capacity of multipotent differentiation into adipogenic, osteogenic, and chondrogenic lineages were determined in pursuance of standard requirements and differentiation protocols.

Adipogenic Differentiation

Cells were seeded at a density of 1.5×10^5 cells/well in 6-well plates, cultured in a complete medium until they reached subconfluence (1–3 days). The culture was then treated with the adipogenic-induction medium containing DMEM supplemented with glucose (1 g/L; Biochrom, FG0415), dexamethasone (final concentration 1 μM, Sigma, D4902), indometacin (final concentration 60 μM, Sigma-Aldrich, I7378-5G), IBMX (final concentration 0.5 mM, Biosource, PHZ 11244), 20% fetal bovine serum (Biochrom, S0615) and 1% penicillin/streptomycin/amphotericin (Biological Industries, 03–033-1B) for 3 weeks, until lipid droplets became visible in cultured cells. Control cells were simultaneously cultured in the complete proliferation medium. Adipogenic and control medium was changed twice a week.

Osteogenic Differentiation

Cells were seeded at a density of 7×10^4 cells/well in 6-well plates, cultured in a complete medium until reaching subconfluence (1–3 days), then treated with the osteogenic-induction medium containing DMEM supplemented with glucose (4.5 g/L; Biochrom, FG0445), dexamethasone (final concentration 0.1 μM, Sigma, D4902), ascorbic acid (final concentration 50 μg/mL, Sigma, A4544-100G), 10% fetal bovine serum (Biochrom, S0615), and 1% penicillin/streptomycin/amphotericin (Biological Industries, 03–033-1B). After 3 days from the beginning of differentiation β-glycerophosphate (Santa Cruz, Sc-220452) was added into the osteogenic-induction medium (final concentration 10 mM) and differentiation was prolonged for 3 weeks. Control cells were simultaneously cultured in the complete proliferation medium. Osteogenic and control growing media were changed twice a week.

Chondrogenic Differentiation

For chondrogenic differentiation 2.5×10^5 trypsinized cells were suspended in 1 mL of the differentiation medium containing DMEM supplemented with glucose (4.5 g/L; Biochrom, FG0445), proline (final concentration 0.35 mM, Carl Roth, 1713.1), dexamethasone (final concentration 0.1 μM, Sigma, D4902), ascorbic acid (final concentration 0.17 mM, Sigma, A4544-100G), TGFβ3 (final concentration 10 μg/mL, Invitrogen, PHG9305), 1% penicillin/streptomycin/amphotericin (Biological Industries, 03–033-1B), and 1% Insulin-Transferrin-Selenium (Gibco, 51500056), placed into 15-mL polypropylene tubes and centrifuged for 5 min at 500*g*. The

caps of the tubes were loosened to permit gas exchange, and the tubes were maintained at 37°C in 5% CO_2. Cells detached from the tube bottom and formed spherical aggregates overnight. Medium was changed 2–3 times a week. The aggregates were harvested at 21st day and prepared for histological analysis.

Assessment of Synovial MSC

SMSC isolated from the synovium were tested for MSC minimal criteria, proposed by The International Society for Cellular Therapy (ISCT). The population of cells could be qualified as MSC, if they satisfy three standard criteria: (a) they must be plastic adherent under standard culture cultivation conditions, (b) they should express CD73, CD90, and CD105, and lack the expression of CD14, CD34, CD45 or CD11b, CD79a or CD19, and HLA class II surface molecules, and (c) they should possess tripotential mesodermal differentiation capability (18). Abundant (higher than 90% of cells) expression, of surface markers characteristic for human MSC, including CD73 (BD Pharmingen, 561254), CD90 (Biolegend, 328108), and CD105 (Invitrogen, MHCD10505), has been detected in both groups of cells. Expression for hematopoietic stem cells markers such as CD34 (Biolegend, 343506), CD45 (Santa Cruz, sc-70686), and CD14 (Biolegend, 301808), HLA DR (Biolegend, 307604) was lower than 5%. No subpopulations according to these markers, as well as to forward scattering (FSC) or side scattering (SSC) were determined in RA or OA SMSC. All cell samples involved in this study were checked to be positive for another fundamental stem-like property, the capacity of multipotent differentiation into adipogenic, osteogenic, and chondrogenic lineages (Fig. 1 as representative case).

Phenotypic Characterization

For phenotypic characterisation of SMSC, 24 surface markers, including adhesion molecules (CD29; CD44; CD49e; CD56; CD106; and CD146); immune system related molecules (CD10; CD36; CD47; CD55; CD182; and CD184); growth factor receptors (CD117; CD221; CD140a; CD140b; CD271; and CD292), and other markers associated with the stemness and/or malignancy-related properties of different cells (CD81; CD133; CD318; CD338; CD349; and STRO-1) were analyzed. After counting, the cells were resuspended in 150 mL of 1% phosphate-buffered saline (PBS)/bovine serum albumin (BSA) and stained for surface structures with the commercially available fluorochrome-labelled antibodies (Table 1) or corresponding isotype controls for 30 min at 4°C in darkness. After incubation cells were washed twice with 1% PBS/BSA and stained with 7-AAD (BD Pharmingen, 559925) for 20 min to exclude dead cells, then were analyzed with flow cytometer FACS Aria, (BD Live Sciences, San Jose). Dead cells and debris were excluded by common gating procedures. Evaluation of flow cytometry data was performed using a "cumulative subtraction" method (19). Ten thousand-gated events were used for the drawing of the histograms.

Protoporphyrin IX Fluorescence Detection

The fluorescence of PpIX in SMSC was determined using a flow cytometer at the spectral region of 695 ± 20 nm, which corresponds to a second peak of a PpIX spectrum (20), under excitation with an argon ion laser (at 488 nm). To follow the time-dependent accumulation of endogenous PpIX in SMSC, the fluorescence intensity was measured at 4, 8, 24, and 48 h after administration of 0.1 and 0.5 mM ALA (Sigma Aldrich,

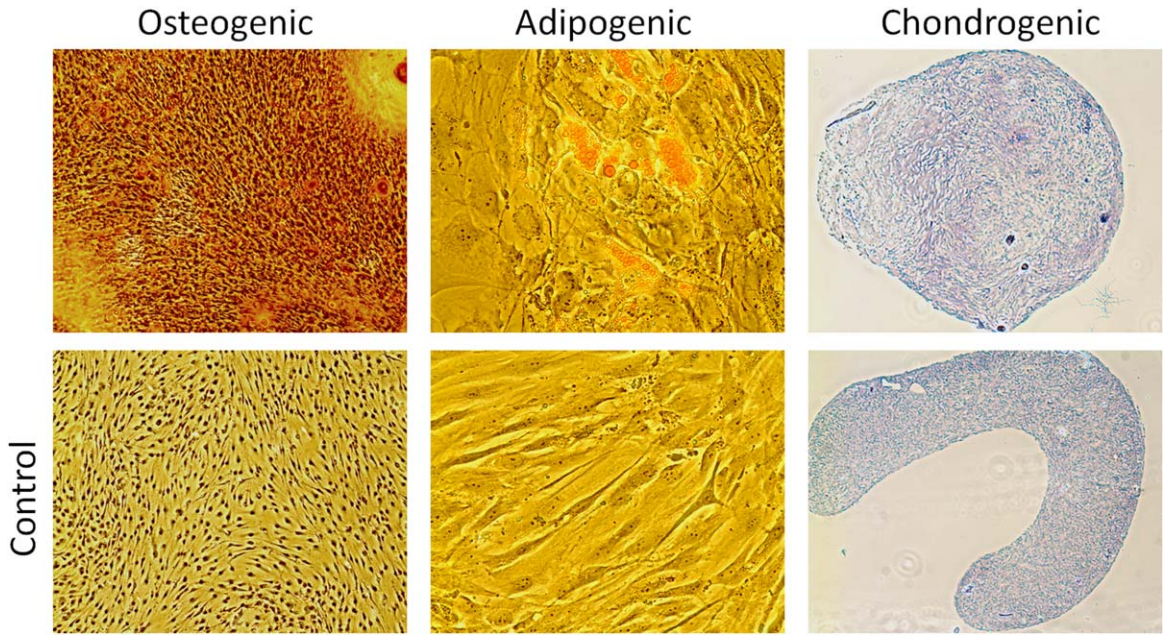

Figure 1. Multipotent differentiation capacity of synovial cells. Osteogenic differentiation: mineralization was stained with Alizarine-red (original magnification ×40); adipogenic differentiation: fat droplets stained with Oil red—O (original magnification ×200) and chondrogenic differentiation: glycosaminoglycans (GAGs) were stained with toluidine blue (original magnification ×40). [Color figure can be viewed in the online issue, which is available at wileyonlinelibrary.com.]

Table 1. Expression ratios of 21 SMSC surface markers. Data are presented as mean ± standard deviation

CD	ANTIGEN	%	LABELING	ISOTYPE	SOURCE
29	Integrin beta-1	98 ± 1	APC	Mouse IgG1	Exbio, 1A-219-T100
36	Glycoprotein IV (GPIV)	1.6 ± 0.9	APC	Mouse IgM, κ	BD Pharmingen, 550956
44	H-CAM	98 ± 2	FITC	Mouse IgG2b	BD Pharmingen, 555478
49e	Integrin alpha-5 chain (VLA-1α)	94.2 ± 17.8	PE	Mouse IgG1	BD Pharmingen, 555617
55	Complement decay-accelerating factor (DAF)	90.8 ± 5.2	APC	Mouse IgG2a	BD Pharmingen, 555696
56	Neural Cell Adhesion Molecule (NCAM)	3.2 ± 1.3	APC	Mouse IgG1	BD Pharmingen, 555518
81	Target of the antiproliferative antibody 1 TAPA-1	98 ± 2	APC	Mouse IgG1	BD Pharmingen, 551112
106	Vascular cell adhesion protein 1 (VCAM-1)	30.0 ± 14.5	APC	Mouse IgG1	BD Pharmingen, 551147
117	Mast/stem cell growth factor receptor SCFR	2.5 ± 2.8	APC	Mouse IgG1	Biolegend, 313206
133	PROML1	0.6 ± 0.6	APC	Mouse IgG1	Miltenyi Biotec, 130-090-826
140a	The platelet-derived growth factor-α receptor (PDGFαR)	5.2 ± 11.0	PE	Mouse IgG2a	Santa Cruz, sc-32287
140b	The platelet-derived growth factor-β receptor (PDGFβR)	71.8 ± 12.3	APC	Mouse IgG1	Biolegend, 323608
146	MCAM	0.3± 0.4	FITC	Mouse IgG1	Santa Cruz, sc-18837
182	Interleukin 8 receptor, beta (CXR2)	0.7 ± 0.8	FITC	Mouse IgG1	BD Pharmingen, 551126
184	C-X-C chemokine receptor type 4 CXR4	3.9 ± 5.1	APC	Mouse IgG2a	Biolegend, 306510
221	Insulin-like Growth Factor 1 (IGF-1) Receptor (IGF-1R)	15.5 ± 8.0	PE	Mouse IgG1	BD Pharmingen, 555999
292	Bone morphogenetic protein receptor, type IA (BMPR1A)	4.8 ± 2.7	FITC	Goat IgG	R&D Systems, FAB346F
318	CUB domain-containing protein 1 CDCP1	26.9 ± 16.1	APC	Mouse IgG2b	Biolegend, 324008
338	ATP-binding cassette sub-family G member 2 ABCG2	0.06 ± 0.03	PE	Mouse IgG2b	Biolegend, 332008
349	Frizzled homolog 9	94.0 ± 3.3	Alexa Fluor® 647	Mouse IgM	Biolegend, 326706
–	Stro-1	3.9 ± 2.1	PE	Mouse IgM	Santa Cruz, sc-47733

Data are presented as mean ± standard deviation.

5451–09-2). Experiments were performed on 2×10^5 cells per well, which corresponds to 95% of confluence. Cells were seeded into a 12-well plate in a complete culturing DMEM for 12 h until incubation with ALA. Nonadherent cells were removed and the medium was changed with the Tyrode's solution, which was prepared by dissolving 8 g NaCl, 0.2 g KCl, 0.2 g $CaCl_2$, 0.21 g $MgCl_2 \cdot 6H_2O$, 0.05 g NaH_2PO_4, 1 g $NaHCO_3$, and 1 g glucose in 1 dm^3 of deionized water without serum and antibiotics. After incubation with 5-ALA the medium was removed, cells were washed three times with PBS and resuspended in 400 μL of 1% PBS/BSA.

Proliferation Analysis

SMSC proliferation analysis was performed using Cell counting Kit-8 (Dojindo, CK04-01) based on reduction of WST-8 [2-(2-methoxy-4-nitrophenyl)−3–(4-nitrophenyl)−5–(2,4-disulfophenyl)−2H-tetrazolium, monosodium salt] by dehydrogenases in the cells producing an orange-colored formazan, which is soluble in the tissue culture medium. The amount of the formazan dye in samples of cells is directly proportional to the number of living cells. Five thousand six hundred cells per well (in duplicates) were seeded in a 96-well plate. After 2, 4, 6, and 8 days in standard cell culture cultivation conditions, the cells were preincubated 3 h with WST-8 in a humidified incubator (37°C, 5% CO_2), and the absorbance of formazan was measured with a plate reader (Asys UVM 340) at 450 nm.

Statistical Analysis

Statistical analysis was done with OriginPro v.8 software using the nonparametric Mann–Whitney's test. All data were expressed as mean ± SD.

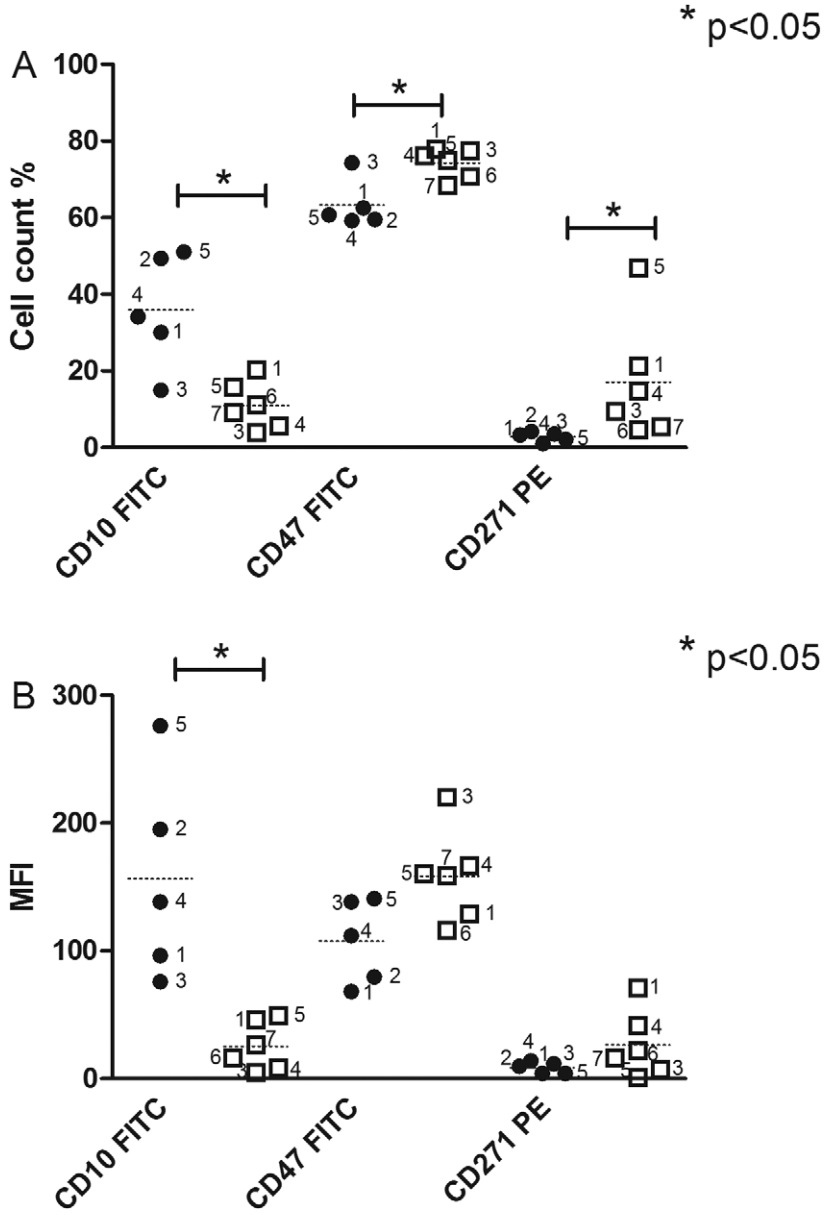

Figure 2. **A** Expression levels of three surface markers in SMSC populations, comprising the RA group (black circles, $n = 5$) and the OA group (white squares, $n = 6$), obtained from flow cytometry data. Values are represented by the mean per sample of SMSC (10^4 events). **B** Mean fluorescence intensity (MFI) of the respective antibody subtracted by the MFI of the respective isotype control. * mark represents statistically significant differences ($P < 0.05$). Supporting information can be found at the flow repository website (https://flowrepository.org/)

Results

Expression of Surface Markers in Synovial MSC

Flow cytometry data were analyzed in relation with the expression of adhesion molecules, immune system related molecules, grow factor receptors, and other cell surface markers, which could be associated with the aggressive phenotype of SMSC in RA. The expression analysis involved 24 surface markers. The expression ratios of 21 markers, which were similar in both OA and RA SMSC groups, are summarized in Table 1. MFI of those markers was also similar in the both groups (data not shown).

High expression level (> 90%) were determined for PDGFβR (CD140b), integrins (CD29, CD49e), hyaluronic acid receptor (CD44), DAF (CD55), CD81, and CD349. While other tested molecules were expressed less frequently. <5% were determined for Glycoprotein IV (CD36), NCAM (CD56), CD117, CD133, MCAM (CD146), CD182, CD184, IGF-1R (CD292), ABCG2 transporter CD338, and Stro-1 (Table 1).

Despite high variation, the statistically significant difference ($P = 0.018$) was found between the average expression levels of surface marker CD10 (Biolegend, 312208)—$35.9 \pm 14.8\%$ in the SMSC of RA group, and much lower

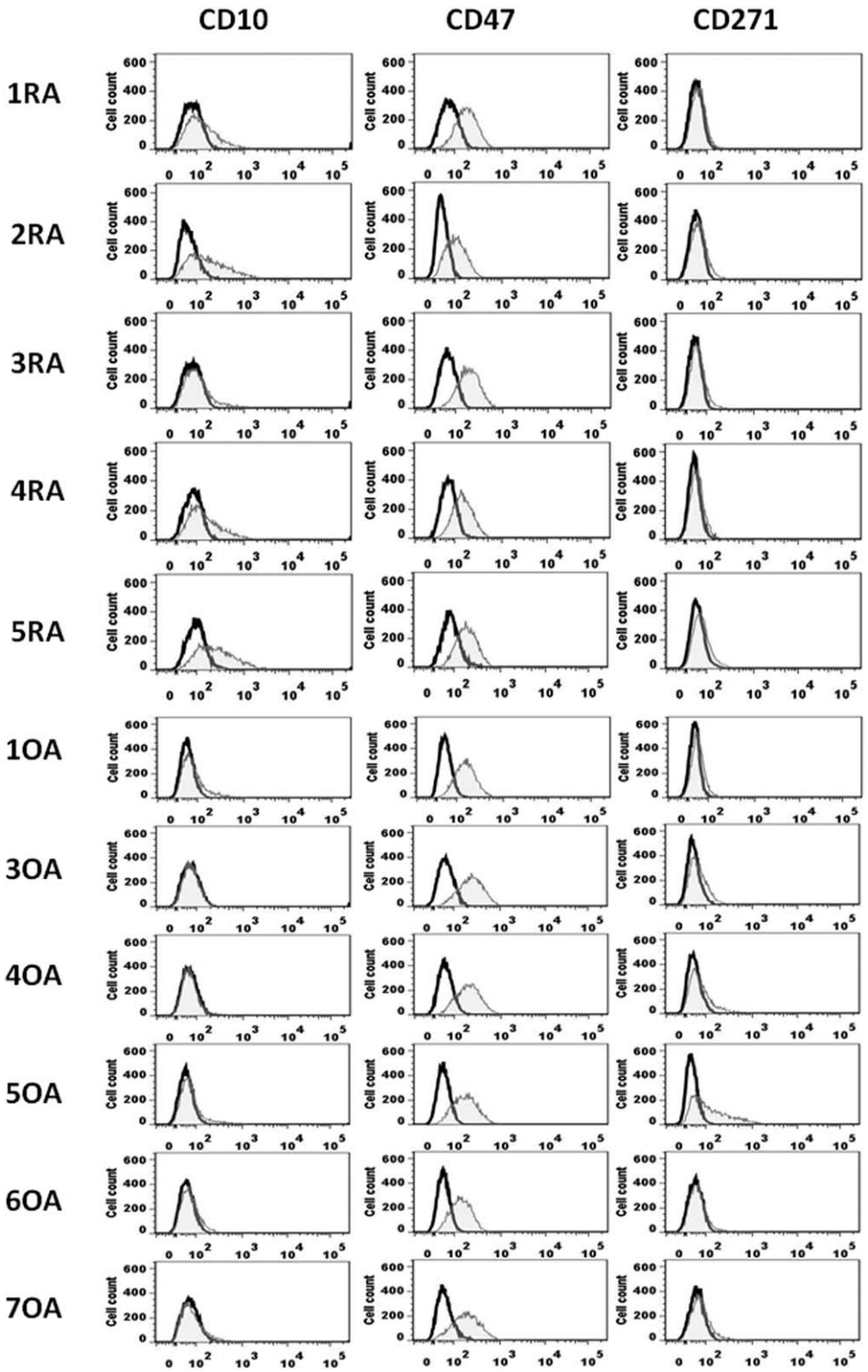

Figure 3. Expression levels of CD10, CD47, and CD271 in SMSC populations stained with commercially available fluorochrome-labelled antibodies (gray color) and corresponding isotype controls (black line). Supporting information can be found at the flow repository website (https://flowrepository.org/)

(10.9 ± 6.2%)—in the OA group. However, the mean expression level of CD271 (Miltenyi Biotec, 130–091-885) in the RA group (2.82 ± 1.25%) was lower ($P = 0.006$) in comparison with the OA (17.09 ± 15.92%) group. In other words, the expression of CD10 was more intensive than the expression of CD271 in the RA SMSC group, while the expression of these

markers in the OA group was less different (Figs 2 and 3) The levels of the cell surface markers CD47 (BD Pharmingen, 556045) were significantly higher ($P = 0.018$) in the case of OA SMSC ($74.3 \pm 3.8\%$) than in the RA SMSC group ($63.3 \pm 6.3\%$; Fig. 2).

PpIX Accumulation in SMSC

Following the administration of 0.1 and 0.5 mM of 5-ALA the PpIX accumulation data of SMSC from RA and OA groups were assessed.

PpIX accumulation was observed since fourth hour of incubation, measuring fluorescence intensity at 4, 8, 24, and 48 h time points (Fig. 4). No PpIX was detected in a control group (without 5-ALA) during the whole observation period. The mean PpIX fluorescence level after incubation with 0.1 mM of 5-ALA was approximately 1.6- to 1.8-fold higher in the RA Group (7,225 and 15,868 a.u., at 4 and 8 h, respectively) in comparison with that of the OA Group (3,963 and 9,426 a.u., at 4 and 8 h, respectively). No statistically significant difference was found between RA and OA groups after incubation with 0.5 and 0.1 mM of ALA-5 (Fig. 4). Noteworthy, incubation with 0.1 mM of 5-ALA enabled to distinguish in either group the particular specimens, bearing capacity to accumulate higher amounts of PpIX, while after incubation with 0.5 mM of 5-ALA, variation between the samples was less evident. However, the PpIX fluorescence intensities in some cases from the RA group (specimens 4RA, 5RA), as well as in the OA group (4OA) were the highest (up to 24 h, Fig. 4A), independently of 5-ALA doses (Fig. 5). The PpIX fluorescence intensity levels for 0.1 and 0.5 mM of 5-ALA in these specimens were similar after 4 and 8 h of incubation. However, concentration related differences were higher for the specimens 2OA, 3OA, 5OA, and 6OA in the OA group (represented by 5 OA in Fig. 5), which showed lower levels of PpIX at lower 5-ALA concentration. Similarly, the specimens 1RA, 2RA, and 3RA from the RA group were characterized by a lower level of fluorescence intensity of PpIX than 4RA and 5RA, however, they accumulated higher levels of PpIX than majority of the specimens from the OA group at certain timepoints, except 4OA (Fig. 4A). The fluorescence intensity of PpIX in the OA group reached a plateau at 24 h after 5-ALA incubation.

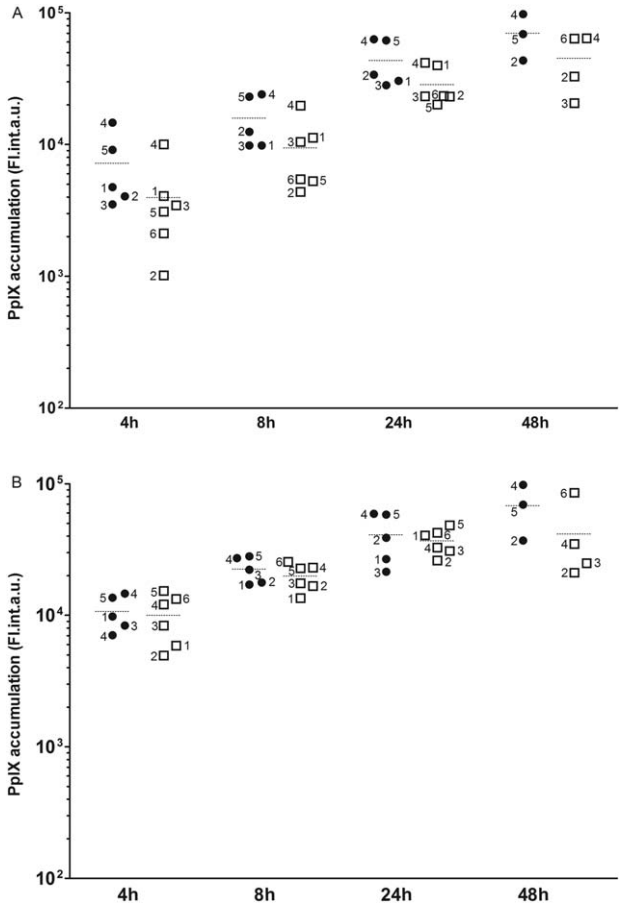

Figure 4. Time-dependent PpIX fluorescence intensity following 0.1 mM (**A**) and 0.5 mM (**B**) administration of 5-ALA. Specimens of SMSC from the RA group are represented as black circles ($n = 5$) and those from the OA group—as white squares ($n = 6$). PpIX fluorescence measurements were performed at 4, 8, 24, and 48 h using a flow cytometer set at 488 nm/695 nm. Values are the mean fluorescence intensities (in arbitrary units, a.u.) per sample of SMSC (10^4 events). Supporting information can be found at the flow repository website (https://flowrepository.org/)

Analysis of PpIX Fluorescence Intensity and Its Relation to the Size and Proliferation Rate of SMSC

As influence of cell size on PpIX production rate has been previously reported (21), the comparison of PpIX accumulation and FSC data was performed. The typical relations between FSC (reflecting cell sizes) and PpIX fluorescence intensity measured for two representative cases from RA and OA groups after 4- and 8-h incubation with 0.1 and 0.5 mM of 5-ALA are presented on Figure 5.

According to FSC data the cells from RA and OA groups were comparable in sizes. No linear dependence between the accumulation of PpIX and the sizes of SMCS was detected for either used 5-ALA concentrations at either observation timepoint (Fig. 5). Two groups of SMSC could be distinguished (e.g., 5OA, 1RA and 4OA, 4RA), which showed slow or fast PpIX accumulation dynamics at 0.1 mM of 5-ALA concentration as well as strong or weak response to the increased 5-ALA concentration, respectively.

Since it has been reported that rapidly proliferating cells with faster metabolism may produce more ALA-derived porphyrins (22), we measured the proliferation intensity of SMSC from RA and OA groups. Proliferation rate was determined by optical density (OD) of accumulation of formazan at 2 days after 4-h incubation with 0.1 mM of 5-ALA. The intensity of OD progressively increased in RA SMSC group. In contrast, a plateau in OA SMSC group was reached after 6 days.

Due to very high interindividual variation of proliferation rates, no statistically significant differences between OD values of RA and OA SMSC groups were detected, although most of RA speciments (1RA, 2RA, 4RA, and 5RA) showed higher proliferation rates than most of OA specimens. (Fig. 6). In some cases from RA or OA SMSC groups (3RA, 5OA,

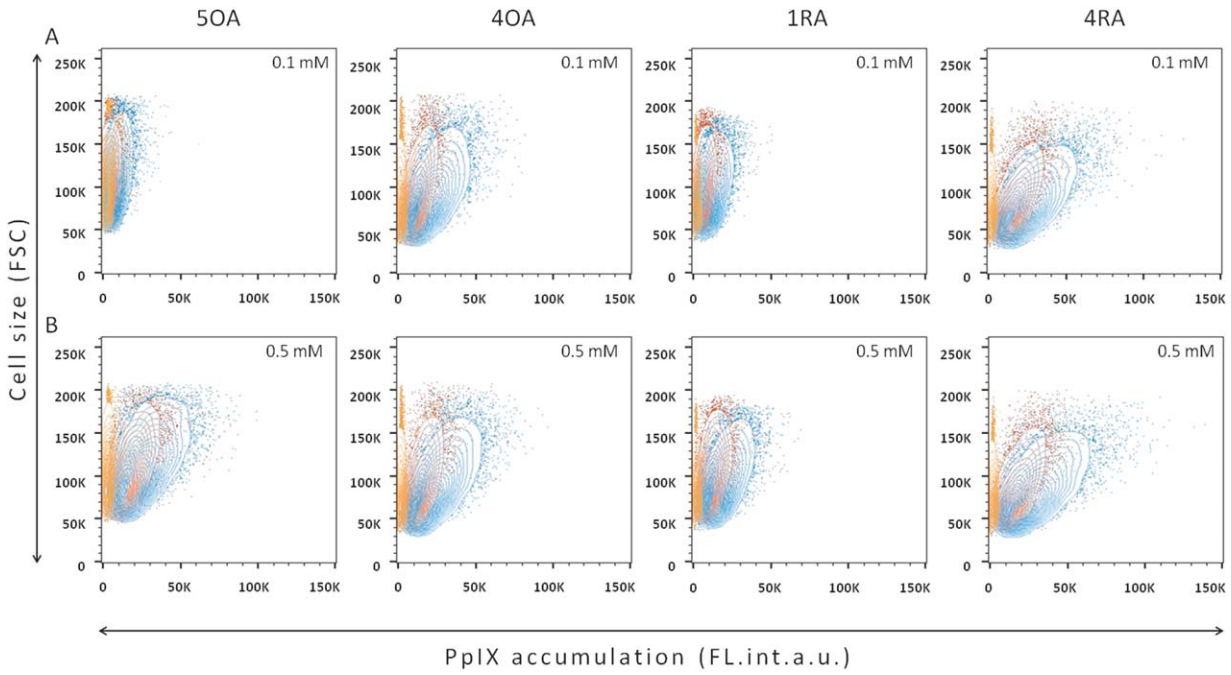

Figure 5. Forward scattering and PpIX fluorescence data from representative specimens of SMSC. The data were collected after 4-h (red dots) and 8-h of (cyan dots) incubation with 0.1 mM (**A**) and 0.5 mM (**B**) of 5-ALA. The orange dots represent data of the control SMSC group at 8 h without 5-ALA administration. 10^4 events were of used for the drawing dot plots. PpIX fluorescence was measured by flow cytometer at ex/em 488/695. [Color figure can be viewed in the online issue, which is available at wileyonlinelibrary.com.]

4RA, 4OA, and 5RA) PpIX accumulation correlated with proliferation rates, but not in the others (1OA, 1RA, 3OA and 2RA).

Discussion

In this study, we observed that mesenchymal cells isolated from both RA and OA synovium expressed the relevant set of surface markers and possessed tripotential mesodermal differentiation capability, which qualify them as SMSC, according to minimal ISCT criteria (18). There is evidence that MSC may be present virtually in any vascularized tissues throughout the whole body (23), and that they respond to inflammatory signals and migrate to injury sites (24). They also exhibit a set of pro-regenerative features that make them attractive agents for both modulation of immune disorders and for regenerative therapy approaches. However, the microenvironments of inflamed synovium share some similarities with that of a cancer and wound, such as pronounced metabolic turnover and proliferating of blood vessels (25). Several studies have revealed that MSC are recruited to cancer and play a particularly important role in disease progression enhancing cancer cell survival and angiogenesis (26,27). It has been also determined that certain growth factors and cytokines present in inflamed tissues may modulate the phenotype of MSC (23) characterized by the altered expression of specific cell surface markers. Therefore, the expression of a panel of selected 24-cell surface markers in SMSC of the RA group has been compared to those of the OA group. Those markers are usually associated with the changed features of the cell, such as the rates of migration and proliferation, differentiation capacity, cell-to-cell interaction. Expression of the majority of the analyzed cell surface markers varied without statistically significant differences between the groups (Table 1). However, SMSC from the RA group had the statistically significantly lower levels of expression for CD47 and CD271, while the higher levels of CD10, as compared to SMSC from the OA group (Fig. 2).

CD47 is an integrin-associated protein (IAP), widely expressed in a majority of normal tissues, suggesting its important role in tissue homeostasis (28). CD47 serves as a "don't eat me" signal and its loss leads to homeostatic phagocytosis of aged or damaged cells (29,30). The role of CD47 in the initiation and persistence of inflammation is still controversial. For instance, the interaction between IAP and thrombospondin-1 is proposed to be a key component of the regulatory circuit involving synovium-derived cells and T lymphocytes, and perpetuates the inflammatory process in the rheumatoid joint (31). Alternatively, CD47/SIRPα interaction is linked to a phenotype of immature APC and the peripheral tolerance under steady state and pathological conditions (32). Moreover, prolonged inflammation has been demonstrated in the CD47-deficient mice (33). These data are in agreement to the lower levels of CD47 expression in SMSC of RA group, observed in our study. Similarly, the expression of CD271, the low-affinity nerve growth factor receptor, characterized as one of basic markers for stromal cells was less expressed in SMSC from the RA group (34). The lower numbers of cells, expressing CD47 and CD271 in the RA group are in agreement with the previous study, reporting negative relationship between chondrogenic and clonogenic capacities of synovial MSC and the magnitude of

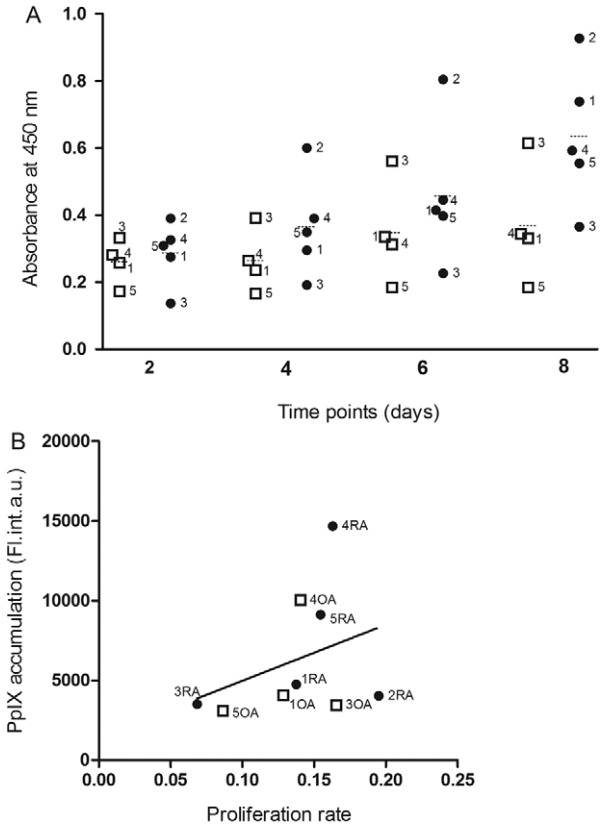

Figure 6. **A** Analysis of SMSC proliferation. Synovium-derived MSC from patients with RA represented as black circles ($n = 5$) and those from patients with OA—as white squares ($n = 4$). Proliferation analysis of SMSC samples of individual patients (5,600 cell per well in 96-well plate). (**B**) Proliferation rate was determined after 2, 4, 6, and 8 days at standard cell culture conditions and expressed as optical density of formazan accumulation. Relationship between SMSC proliferation rate and PpIX accumulation. OD values were normalized to incubation time (2 days).

synovitis in RA (35). Tendency of lower MFI values for those markers might also reflect the impact of highly inflammatory milieu in arthritic joints, which could lead to changes in the phenotype of SMSC such as transition into underdifferentiated precursors of aggressive FLS (36). CD10 is known as a cell surface zinc-dependent metalloproteinase (Mr 90–110 kDa), being a common antigen of an acute lymphoblastic leukaemia. This enzyme causes degradation of the extracellular matrix (ECM), has an activity similar to that of matrix metalloproteinases and may stimulate migration of SMSC similarly as in the case of malignancy. Multiple studies have shown that the increased expression of CD10 in stromal cells is associated with the higher invasiveness of tumors (37–39). Moreover, the expression of CD10 appears to be significantly associated with mutations of *p53* in tumour cells and a larger tumour size, suggesting its possible role in tumor invasion and metastatic capacity (40). Taken together, we determined an altered immunophenotype in SMSC of RA, suggesting their possible implication in maintenance of aggressive synoviocyte population, involved in the cartilage degradation and pannus formation. The observed variation in expression of surface markers CD271, CD10 between SMSC from RA and OA groups does not seem to be caused by age induced changes (28–30). However, such impact cannot be fully rejected due to the scarcity of related evidence, including age-related expression data of CD47.

While the statistical difference between the mean values of PpIX accumulation data in OA and RA groups did not reach the level of significance, the low concentration (0.1 mM) of 5-ALA (Fig. 4A) seemed to be more appropriate to distinguish the specimens in the RA group (4RA, 5RA) and in the OA group (4OA), which accumulated the highest amounts of PpIX during initial hours (4 and 8 h). The applied concentrations of 5-ALA had no influence on PpIX accumulation in those specimens (Figs. 4A and 4B and 5) in contrast to the rest of specimens from the OA and RA groups (represented by 5OA and 1RA, Fig. 5) that showed a stronger dependence on 5-ALA doses. Nevertheless, after 24 h all specimens accumulated similar amounts of PpIX, and the plateau was observed irrespectively of the applied ALA doses (Fig. 4). We suppose that these similarities might be caused by enhanced metabolic activity of stem-like cells present in specimens from both RA and OA groups. The differences between the specimens in the capacity to accumulate PpIX at a low ALA concentration, as well as in the strength of response to an increased ALA concentration could be affected by at least two groups of factors regulating (a) metabolic turnover of PpIX and (b) ALA uptake in SMSC. The former group usually comprises varying capacity of intracellular heme production, iron-dependent feedback control mechanisms, low activity of the enzyme ferrochelatase, and high activity of the enzyme porphobilinogen deaminase (PBGD) (41). The latter group is strongly associated with the availability of cell membrane transporters (42,43). In addition, the similar accumulation of PpIX that was observed in some specimens from RA and OA SMSC groups at initial hours (Fig. 4A) might be related to variations in the level of inflammation in vivo due to prolonged RA treatment. Another group of factors that might have an effect on intracellular accumulation of PpIX under the same confluence conditions include the rate of proliferation and the size of cells (44). The analysis of FSC and PpIX accumulation data showed the absence of stickout subpopulations in all specimens (e.g., Fig. 5), excluding the size of cells as a relevant factor to distinguish their capacity to accumulate PpIX in specimens from RA and OA groups (Fig. 4). The comparison between the cell proliferation rates in RA and OA SMSC groups and the corresponding PpIX accumulation data (Fig. 6) led to a similar assumption. In many situations, both cancer cells in vitro and tumor tissue in vivo accumulate substantially more PpIX than the normal cells and tissues (45). However, faster metabolic activity, as well as efficient PpIX production, is not always associated with an increased growth rate of cells. It has been demonstrated that certain growth-arrested, differentiated cells produce more PpIX than their proliferating, undifferentiated counterparts (46). Moreover, the association between PpIX accumulation, the numbers of mitochondria and their activity has been demonstrated (47).

The comparison of the expression levels of CD47, CD271, and CD10, which were significantly different in the

specimens from RA and OA groups and the PpIX fluorescence intensity measured in those specimens at 4and 8 h after 0.1 mM of 5-ALA incubation, did not reveal direct relationship. The accumulation of PpIX was the highest in the specimens 4RA and 5RA from the RA group (Fig.4A), which also showed high-expression levels of CD10 (Fig. 2). The opposite was true for the specimen 3RA. However, the specimen 2RA, which expressed high levels of CD10 and also similar levels of CD47 and CD271 to those found in 5RA, had low PpIX fluorescence intensity. Moreover, the variations in PpIX fluorescence intensities had no reflection in the expression levels of CD47 and CD271 in the same specimens within the groups.

Conclusions

The expression of majority of the 24 tested SMSC surface markers varied from low to high levels without statistically significant difference between RA and OA groups. However, the levels of the immunologically active CD47 and the grow factor receptor CD271 were significantly lower, while the expression of the cell membrane zinc-dependent metalloproteinase CD10 was more intensive in the RA group of SMSC. No direct association between the expression levels of the three markers (CD47, CD271, and CD10) and the PpIX fluorescence was observed and comparison of the mean intensities of PpIX fluorescence revealed no statistically significant differences between the RA and OA groups. Noteworthy, some conspicuous distinction in PpIX accumulation was observed in certain specimens within these groups at initial hours of incubation with the lower (0.1 mM) 5-ALA concentration, suggesting possibilities of this method application for the characterization of individual SMSC populations.

Literature Cited

1. Neumann E, Lefevre S, Zimmermann B, Gay S, Muller-Ladner U. Rheumatoid arthritis progression mediated by activated synovial fibroblasts. Trends Mol Med 2010;16:458–468.
2. Treese C, Mittag A, Lange F, Tarnok A, Loesche A, Emmrich F, Lehmann J, Sack U. Characterization of fibroblasts responsible for cartilage destruction in arthritis. Cytometry Part A 2008;73A:351–360.
3. Tak PP, Smeets TJ, Daha MR, Kluin PM, Meijers KA, Brand R, Meinders AE, Breedveld FC. Analysis of the synovial cell infiltrate in early rheumatoid synovial tissue in relation to local disease activity. Arthritis Rheum 1997; 40:217–225.
4. Lefevre S, Knedla A, Tennie C, Kampmann A, Wunrau C, Dinser R, Korb A, Schnaker EM, Tarner IH, Robbins PD, et al. Synovial fibroblasts spread rheumatoid arthritis to unaffected joints. Nat Med 2009;15:1414–1420.
5. Bartok B, Firestein GS. Fibroblast-like synoviocytes: key effector cells in rheumatoid arthritis. Immunol Rev 2010;233:233–255.
6. van der Pouw Kraan TC, van Gaalen FA, Kasperkovitz PV, Verbeet NL, Smeets TJ, Kraan MC, Fero M, Tak PP, Huizinga TW, Pieterman E, et al. Rheumatoid arthritis is a heterogeneous disease: evidence for differences in the activation of the STAT-1 pathway between rheumatoid tissues. Arthritis Rheum 2003; 48:2132–2145.
7. Chen FH, Tuan RS. Mesenchymal stem cells in arthritic diseases. Arthritis Res Therapy 2008; 10:223
8. Kastrinaki MC, Sidiropoulos P, Roche S, Ringe J, Lehmann S, Kritikos H, Vlahava VM, Delorme B, Eliopoulos GD, Jorgensen C, et al. Functional, molecular and proteomic characterisation of bone marrow mesenchymal stem cells in rheumatoid arthritis. Ann Rheum Dis 2008; 67:741–749.
9. Papadopoulou A, Yiangou M, Athanasiou E, Zogas N, Kaloyannidis P, Batsis I, Fassas A, Anagnostopoulos A, Yannaki E. Mesenchymal stem cells are conditionally therapeutic in preclinical models of rheumatoid arthritis. Ann Rheum Dis 2012; 71: 1733–1740.
10. Bagdonas S, Kirdaite G, Streckyte G, Graziene V, Leonaviciene L, Bradunaite R, Venalis A, Rotomskis R. Spectroscopic study of ALA-induced endogenous porphyrins in arthritic knee tissues: targeting rheumatoid arthritis PDT. Photochem Photobiol Sci 2005; 4:497–502.
11. Kennedy JC, Pottier RH, Pross DC. Photodynamic therapy with endogenous protoporphyrin IX: basic principles and present clinical experience. J Photochem Photobiol B Biol 1990; 6:143–148.
12. Fotinos N, Campo MA, Popowycz F, Gurny R, Lange N. 5Aminolevulinic acid derivatives in photomedicine: characteristics, application and perspectives. Photochem Photobiol 2006; 82:994–1015.
13. Kirdaite G, Lange N, Busso N, Van Den Bergh H, Kucera P, So A. Protoporphyrin IX photodynamic therapy for synovitis. Arthritis Rheum 2002; 46:1371–1378.
14. Rudys R, Kirdaite G, Bagdonas S, Leonaviciene L, Bradunaite R, Streckyte G, Rotomskis R. Spectroscopic assessment of endogenous porphyrins in a rheumatoid arthritis rabbit model after the application of ALA and ALA-Me. J Photochem Photobiol B Biol 2013; 119:15–21.
15. Collaud S, Juzeniene A, Moan J, Lange N. On the selectivity of 5-aminolevulinic acid-induced protoporphyrin IX formation. Curr Med Chem Anticancer Agents 2004; 4:301–316.
16. Altman R, Asch E, Bloch D, Bole G, Borenstein D, Brandt K, Christy W, Cooke TD, Greenwald R, Hochberg M, et al. Development of criteria for the classification and reporting of osteoarthritis. Classification of osteoarthritis of the knee. Diagnostic and Therapeutic Criteria Committee of the American Rheumatism Association. Arthritis Rheum 1986; 29:1039–1049.
17. Arnett FC, Edworthy SM, Bloch DA, McShane DJ, Fries JF, Cooper NS, Healey LA, Kaplan SR, Liang MH, Luthra HS, et al. The American Rheumatism Association 1987 revised criteria for the classification of rheumatoid arthritis. Arthritis Rheum 1988; 31:315–324.
18. Dominici M, Le Blanc K, Mueller I, Slaper-Cortenbach I, Marini F, Krause D, Deans R, Keating A, Prockop D, Horwitz E. Minimal criteria for defining multipotent mesenchymal stromal cells. The International Society for Cellular Therapy position statement. Cytotherapy 2006; 8:315–317.
19. Overton WR. Modified histogram subtraction technique for analysis of flow cytometry data. Cytometry 1988; 9:619–626.
20. Rudys R, Denkovskij J, Kirdaite G, Bagdonas S. Induction of protoporphyrin IX in patient-derived synoviocytes, cartilage explants and chondrons after application of 5-aminolevulinic acid or its methyl ester. J Photochem Photobiol B Biol 2014; 141: 228–234.
21. Gibbs SL, Chen B, O'Hara JA, Hoopes PJ, Hasan T, Pogue BW. Protoporphyrin IX level correlates with number of mitochondria, but increase in production correlates with tumor cell size. Photochem Photobiol 2006; 82:1334–1341.
22. Pourzand C, Reelfs O, Kvam E, Tyrrell RM. The iron regulatory protein can determine the effectiveness of 5-aminolevulinic acid in inducing protoporphyrin IX in human primary skin fibroblasts. J Invest Dermatol 1999; 112:419–425.
23. Lv FJ, Tuan RS, Cheung KM, Leung VY. Concise review: the surface markers and identity of human mesenchymal stem cells. Stem Cells 2014; 32:1408–1419.
24. Sohni A, Verfaillie CM. Mesenchymal stem cells migration homing and tracking. Stem Cells Int 2013; 2013:130763
25. Raatz Y, Ibrahim S, Feldmann M, Paleolog EM. Gene expression profiling and functional analysis of angiogenic markers in murine collagen-induced arthritis. Arthritis Res Therapy 2012; 14:R169
26. Stagg J. Mesenchymal stem cells in cancer. Stem Cell Rev 2008; 4:119–124.
27. Kuhn NZ, Tuan RS. Regulation of stemness and stem cell niche of mesenchymal stem cells: implications in tumorigenesis and metastasis. J Cell Physiol 2010; 222:268–277.
28. Reinhold MI, Lindberg FP, Plas D, Reynolds S, Peters MG, Brown EJ. In vivo expression of alternatively spliced forms of integrin-associated protein (CD47). J Cell Sci 1995; 108:3419–3425.
29. Blazar BR, Lindberg FP, Ingulli E, Panoskaltsis-Mortari A, Oldenborg PA, Iizuka K, Yokoyama WM, Taylor PA. CD47 (integrin-associated protein) engagement of dendritic cell and macrophage counterreceptors is required to prevent the clearance of donor lymphohematopoietic cells. J Exp Med 2001; 194:541–549.
30. Gardai SJ, McPhillips KA, Frasch SC, Janssen WJ, Starefeldt A, Murphy-Ullrich JE, Bratton DL, Oldenborg PA, Michalak M, Henson PM. Cell-surface calreticulin initiates clearance of viable or apoptotic cells through trans-activation of LRP on the phagocyte. Cell 2005; 123:321–334.
31. Vallejo AN, Yang H, Klimiuk PA, Weyand CM, Goronzy JJ. Synoviocyte-mediated expansion of inflammatory T cells in rheumatoid synovitis is dependent on CD47-thrombospondin 1 interaction. J Immunol 2003; 171:1732–1740.
32. Toledano N, Gur-Wahnon D, Ben-Yehuda A, Rachmilewitz J. Novel CD47: SIRPalpha dependent mechanism for the activation of STAT3 in antigen-presenting cell. PloS One 2013; 8:e75595
33. Lamy L, Foussat A, Brown EJ, Bornstein P, Ticchioni M, Bernard A. Interactions between CD47 and thrombospondin reduce inflammation. J Immunol 2007; 178: 5930–5939.
34. Arufe MC, De la Fuente A, Fuentes I, de Toro FJ, Blanco FJ. Chondrogenic potential of subpopulations of cells expressing mesenchymal stem cell markers derived from human synovial membranes. J Cell Biochem 2010; 111:834–845.
35. Jones E, Churchman SM, English A, Buch MH, Horner EA, Burgoyne CH, Reece R, Kinsey S, Emery P, McGonagle D, et al. Mesenchymal stem cells in rheumatoid synovium: enumeration and functional assessment in relation to synovial inflammation level. Ann Rheum Dis 2010; 69:450−457.
36. Li X, Makarov SS. An essential role of NF-kappaB in the "tumor-like" phenotype of arthritic synoviocytes. Proc Natl Acad Sci USA 2006; 103:17432–17437.
37. Huang WB, Zhou XJ, Chen JY, Zhang LH, Meng K, Ma HH, Lu ZF. CD10-positive stromal cells in gastric carcinoma: correlation with invasion and metastasis. Jpn J Clin Oncol 2005; 35:245–250.
38. Makretsov NA, Hayes M, Carter BA, Dabiri S, Gilks CB, Huntsman DG. Stromal CD10 expression in invasive breast carcinoma correlates with poor prognosis, estrogen receptor negativity, and high grade. Mod Pathol 2007; 20:84–89.
39. Voutsadakis IA, Vlachostergios PJ, Daliani DD, Karasavvidou F, Kakkas G, Moutzouris G, Melekos MD, Papandreou CN. CD10 is inversely associated with

nuclear factor-kappa B and predicts biochemical recurrence after radical prostatectomy. Urol Int 2012; 88:158–164.

40. Ogawa H, Iwaya K, Izumi M, Kuroda M, Serizawa H, Koyanagi Y, Mukai K. Expression of CD10 by stromal cells during colorectal tumor development. Hum Pathol 2002; 33:806–811.
41. Peng Q, Warloe T, Berg K, Moan J, Kongshaug M, Giercksky KE, Nesland JM. 5Aminolevulinic acid-based photodynamic therapy. Clinical research and future challenges. Cancer 1997; 79:2282–2308.
42. Rud E, Gederaas O, Hogset A, Berg K. 5aminolevulinic acid, but not 5-aminolevulinic acid esters, is transported into adenocarcinoma cells by system BETA transporters. Photochem Photobiol 2000; 71:640–647.
43. Neumann J, Brandsch M. Delta-aminolevulinic acid transport in cancer cells of the human extrahepatic biliary duct. J Pharmacol Exp Ther 2003; 305:219–224.
44. Cunderlikova B, Peng Q, Mateasik A. Factors implicated in the assessment of aminolevulinic acid-induced protoporphyrin IX fluorescence. Biochim Biophys Acta 2013; 1830:2750–2762.
45. Momma T, Hamblin MR, Hasan T. Hormonal modulation of the accumulation of 5-aminolevulinic acid-induced protoporphyrin and phototoxicity in prostate cancer cells. Int J Cancer 1997; 72:1062–1069.
46. Ortel B, Sharlin D, O'Donnell D, Sinha AK, Maytin EV, Hasan T. Differentiation enhances aminolevulinic acid-dependent photodynamic treatment of LNCaP prostate cancer cells. Br J Cancer 2002; 87:1321–1327.
47. Gibson SL, Nguyen ML, Havens JJ, Barbarin A, Hilf R. Relationship of delta-aminolevulinic acid-induced protoporphyrin IX levels to mitochondrial content in neoplastic cells in vitro. Biochem Biophys Res Commun 1999; 265: 315–321.